Biophysical Chemistry, 48 (1994) 321–336
Elsevier Science B.V., Amsterdam

BIOCHE 01835

Light intensity distribution in thylakoids and the polarity of the photovoltaic effect

Géza Meszéna

Department of Atomic Physics, Eötvös University, Puskin u. 5–7., Budapest, 1088 (Hungary)

Hans V. Westerhoff

Division of Molecular Biology, The Netherlands Cancer Institute, Plesmanlaan 121, 1066 CX Amsterdam (The Netherlands)
and
E.C. Slater Institute, University of Amsterdam, Plantage Muidergracht 12, 1018 Amsterdam (The Netherlands)

(Received 10 May 1993; accepted 1 August 1993)

Abstract

The spatial organization in photosystems containing chloroplast membranes is such that some of the relevant distances are of the order of the wavelength of the absorbed light. Consequently, interference between incident and reflected light may occur. This paper calculates the heterogeneity to be expected in the resultant light intensity. The pattern is determined by the wavelength-dependent phase shift of light during scattering. We show that in stroma-membranes this heterogeneity may well be responsible for paradoxical polarities of the photovoltaic effect in which flash illumination of a chloroplast suspension generates a macroscopic electric potential opposite to that expected from shading. The grana-stack dimensions are calculated to lead to the classical picture of shading, consistent with a "normal" photovoltaic effect. We demonstrate that the simultaneous presence of stroma- and grana-membranes may explain the observed wavelength dependence of the polarity of the photovoltaic effect.

Keywords: Chloroplasts; Heterogeneity; Membranes; Photovoltaic effect

1. Introduction

The light reactions of the photosynthesis in green plants take place in a complicated membrane structure within the chloroplasts [1,2]. About 1000, interconnected, disk-shaped compartments with a diameter of about 500 nm constitute the thylakoids. In some regions thylakoid membranes are stacked forming the so-called grana-stacks. (Unstacked thylakoid regions constitute the stroma-thylakoid or stroma-membrane.) The physiological role of the difference between grana and the stroma-thylakoid is not known although their relative contents of the two photosystems and H^+–ATPase differ [3]. Because of the presence of the various membranes, at the distances of the order of the wavelength of the exciting light, a complex pattern of diffraction and interference is to be expected in this system. We here address the question of the resulting distribution of light intensity. Light intensity distribution in the thylakoid structure is related to

SSDI 0301-4622(93)E0089-N

the polarity of macroscopic photovoltaic effects of a chloroplast suspension and to the free energy transduction efficiency of the chloroplast.

The very first step of the photosynthetic energy transformation is a charge separation in the photosynthetic reaction center. This microscopic charge transfer can be detected macroscopically as a transient voltage (the photovoltage) between two electrodes immersed into a chloroplast suspension that is subjected to a light flash [4–6]. The existence of the macroscopic signal depends on the uneven distribution of the light in the thylakoid system. (If the light intensity was the same at the two sides of each vesicle, the voltages generated by the opposite sides would cancel each other.) It is well established, that during the charge separation an electron moves from the inside to the outside of the thylakoid vesicle. If the side of a thylakoid vesicle that is closest to the light source is subject to a higher light intensity than the side farther away from that light source, the illuminated vesicle should generate an electric potential positive at the side farthest away from the light source. Since the same holds for all vesicles in the suspension, the electrode the farther from the light source should become positive. In the following we refer to this polarity as positive. This polarity was found in the early experiments with white light pulses coming from a flash lamp [4–6], as well as in an experiment with laser excitation [7]. In line with this, so-called, "light gradient theory" the signal vanished at saturating light intensity, i.e. when a minor difference between light intensities does not lead to a difference in charge transfer rates.

However, the polarity of the macroscopic photovoltage was negative in many other experiments and the origin of the different polarities was debated [8–10]. As we showed in the accompanying article, the polarity is determined solely by the wavelength of the exciting light [11]. Roughly speaking, polarity is positive at the blue and red absorption bands of chlorophyll, negative between them and negative at wavelengths above 700 nm. There is also a wavelength region where the photovoltage exhibits two polarities differing kinetically. Neither the photovoltage of negative polarity, nor the wavelength dependence of the polarity can be accounted for by the original explanation.

To explain this wavelength dependence a modified version of the light-gradient theory was proposed by Meszéna and DeVault [10]. According to these authors, wavelength-dependence of the light-distribution is responsible for the wavelength-dependent polarity. Since the geometrical dimensions of the thylakoid vesicle system are in or below the range of the wavelength of the absorbed light, it is insufficient to reason in the terms of geometrical optics and suppose that the one side of the vesicle simply shades the other one. Within the lamella system the light should be subject to optical interference [10].

In this paper we develop the modified light-gradient theory in quantitative terms and show that it explains at least qualitatively the reported wavelength dependence of the photovoltaic effect. We calculate the light-intensity distribution in the stroma-thylakoid as well as in the grana, and compare our results to the photovoltage data.

2. Results

2.1. Theoretical background

The fact that the photovoltage signal is positive within chlorophyll and carotenoid absorption bands and negative outside them suggests that the complex polarizability (e.g. the absorbance and the refractive index) of the pigments has a crucial role in determining the interference pattern. In other words, the wavelength-dependent phase of the scattered light (relative to the incident light) determines the interference pattern in the thylakoid system.

In classical electrodynamics interaction of light and matter is described in the following way [12]. The electric field of the light forces the molecular charge distribution to oscillate. The resulting oscillating dipoles reemit light in all directions. In the inhomogeneous case of particles in a medium, emitted light is observed as scattered light from a distance much larger than the size of the scattering piece of material. Inside a continuous medium

both absorption and refraction are the consequences of the interference between the incident and the emitted light. In that context the emitted light is usually not referred to as scattered. To avoid any confusion we will use the term "reemitted light" to refer to the waves that are responsible for scattering as well as refraction and absorption. Inside an inhomogeneous structure the outcome of this interference is more complicated. To interpret the interference pattern as a combined effect of scattering, refraction and absorption, is not necessary and straightforward.

Since we are interested in the light distribution pattern in the direction of the incident light, we restrict this paper to the one-dimensional case. Accordingly, we approximate the thylakoids as a set of infinite sheets. This allows us to use an elegant way to describe the interaction of electromagnetic waves and matter developed by Feynman and Orear [13] rather than employing the complicated formulas of scattering theory. In this method a sheet rather than a molecule is regarded as a unit of description: the sheet has an oscillating and, consequently radiating dipole-moment density. The bonus is that we shall not have to calculate the wave radiated by the sheet as a superposition of the waves emitted by the individual atoms in it.

By way of illustration, the reemitted light wave is calculated in Appendix A for the case of a single absorption line. Our ultimate calculations are based on the empirical absorption spectrum and the Kramers–Kronig relation [12]. The connection between the reemission coefficient of a single sheet and the absorbance and refractive index of a continuous medium is presented in Appendix B.

2.2. *Light intensity in front of and behind a single sheet of absorbing matter*

We begin by calculating the light intensity in front of and behind a single sheet. We suppose, that the incoming light waves travel perpendicularly to the plain of the sheet. The sheet is perpendicular to the z axis, located at $z = 0$ and thin compared to the wavelength of the light (fig. 1). The incident light propagates in the positive z direction. In complex notation the electric field component of the incoming light reads:

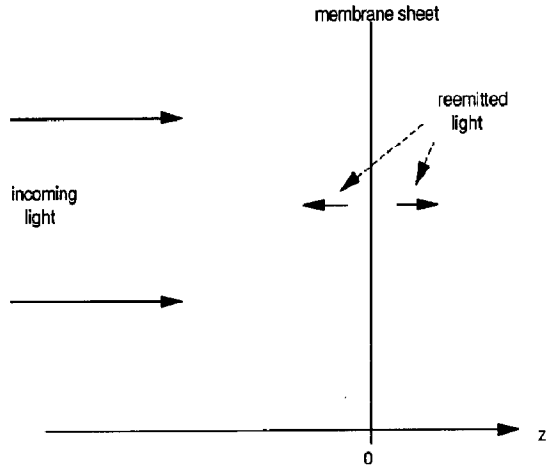

Fig. 1. Interaction of light and a single sheet.

$$E_{in} = E_0 \, e^{ik_w z}, \tag{1}$$

where time dependence $\exp[-i(2\pi c/\lambda)t]$ is omitted and k_w stands for the wave number in the solution,

$$k_w = \frac{2\pi n_w}{\lambda} \tag{2}$$

(λ is the wavelength in vacuum, n_w denotes the refractive index of the aqueous medium.)

This field forces the molecular dipoles to oscillate. The oscillating dipoles (distributed evenly over the sheet) radiate light of the same amplitude and phase in either direction,

$$E_{reem} = \delta \, e^{ik_w|z|} E_0, \tag{3}$$

where

$$\delta = \delta_1 + i\delta_2 = r \, e^{i\varphi} \tag{4}$$

is referred to as reemission coefficient. r is the relative amplitude and ϕ is the phase delay of the reemitted light relative to the incident light.

$$\delta_1 = r \cos \phi,$$
$$\delta_2 = r \sin \phi \tag{5}$$

are the real and the imaginary parts, respectively, of the reemission coefficient. For a biological

membrane $r \ll 1$. (A single sheet of membrane is almost transparent.)

In Appendix A, δ_1 and δ_2 are calculated for the case of a single absorption line. At the absorption maximum δ is negative real, i.e. $\phi \approx 180°$ corresponds to pure absorption. Away from the maximal absorption δ_1 becomes small and the reemitted light becomes out of phase with the incident light. The sign of δ_2 is opposite at the two sides of the absorption band. It is positive ($\phi \approx 90°$) for frequencies smaller, while negative ($\phi \approx 270°$) for frequencies larger than the resonance frequency.

The resultant field is

$$E = E_0(e^{ik_w z} + \delta\, e^{ik_w|z|}). \tag{6}$$

Behind the sheet, i.e. for $z > 0$, the incident and the reemitted waves propagate in the same direction,

$$E(z > 0) = E_0(1 + \delta)\, e^{ik_w z}. \tag{7}$$

Consequently, behind the sheet the light will have a phase and amplitude slightly different from the incident ones. Absorbance is a consequence of the destructive interference between the incoming and the reemitted light. The amplitude of the light behind the sheet is $|E| = (1 + \delta_1)E_0$. δ_1 must be negative (otherwise the sheet would amplify, rather than attenuate the light, which would require a source of free energy). Its absolute value equals half the absorbance by the sheet. The refractive index comes from the phase shift of the light caused by interference between the incoming light and the out-of-phase component of the reemitted light. Consequently, it is related to δ_2. (According to eq. (B.8), $n > 1$ for frequencies below the absorption maximum of the medium, because $\delta_2 > 0$ in that case.) The out-of-phase reemission is also responsible for light scattering outside the absorption bands.

In front of the sheet ($z < 0$) the incident and the reemitted waves propagate in opposite directions and give rise to a standing wave interference pattern:

$$\begin{aligned} E(z < 0) &= E_0[e^{-ik_w z} + \delta\, e^{-ik_w z}] \\ &= E_{in}[1 + r\, e^{-i(4\pi n_w(z/\lambda) - \phi)}]. \end{aligned} \tag{8}$$

For the amplitude of the wave at the two sides of the sheet, we find:

$$\begin{aligned} &|E| = E_0(1 + r\cos\phi), \quad \text{for } z > 0, \\ &|E| = E_0\{1 + r\cos[4\pi n_w(z/\lambda) - \phi]\}, \\ &\text{for } z < 0. \end{aligned} \tag{9}$$

($r \ll 1$ was used.) Note, that the amplitude is the same for $z = +0$ and $z = -0$: it is the same immediately in front of and behind the sheet. This conclusion is definitely different from the common sense expectation of sharp intensity change across a thin, but optically dense sheet. In wave optics, everything has to be smooth at scales smaller than the wavelength. This phenomenon has an important consequence for the photovoltage problem: it makes the concept of "shadow" in the original version of the light-gradient theory unreliable.

The full line in fig. 2a illustrates the implications of eq. (9) for light of the wavelength of the absorption maximum. Behind the sheet the intensity is reduced, but in front of the sheet an interference pattern arises averaging around the intensity of the incident light. Figs. 2b and 2c show that far away from the maximum absorption wavelength, the interference pattern in front of the sheet is retained, but shifted relative to that of fig. 2a.

2.3. Calculation of the reemission coefficient, δ

To calculate the light distribution as a function of the wavelength we have to know $\delta_1(\lambda)$ and $\delta_2(\lambda)$. $-\delta_1$ is simply half the absorbance, hence it is known. But δ_2 is very difficult to measure. (It could be calculated from the refractive index of the thylakoid, but no homogeneous sample of the latter is available to measure that refractive index.) Fortunately the real (δ_1) and imaginary (δ_2) part of δ depend on each other through the Kramers–Kronig relations [14,15],

$$\begin{aligned} \delta_1(\omega) &= \frac{1}{\pi}\mathcal{P}\int_{-\infty}^{\infty} \frac{\delta_2(\omega')}{\omega' - \omega}\, d\omega', \\ \delta_2(\omega) &= -\frac{1}{\pi}\mathcal{P}\int_{-\infty}^{\infty} \frac{\delta_1(\omega')}{\omega' - \omega}\, d\omega', \end{aligned} \tag{10}$$

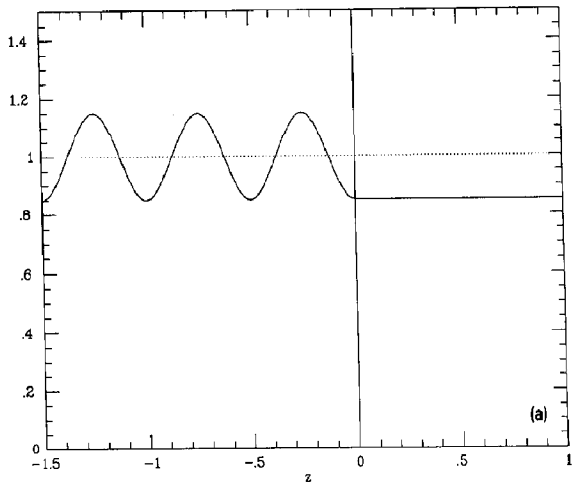

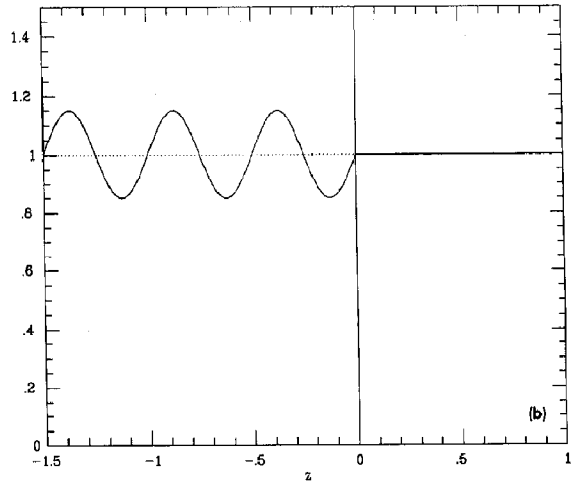

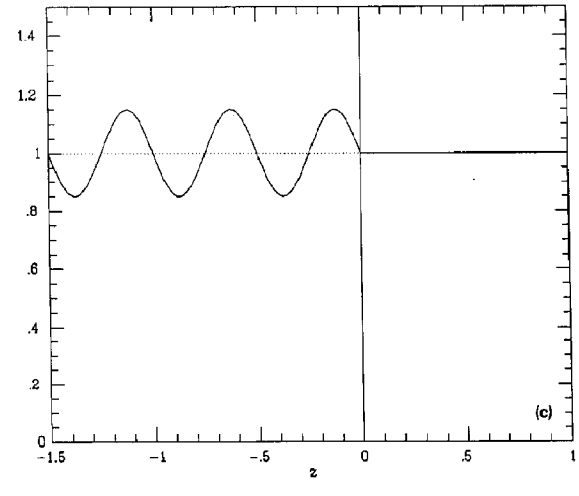

where $\mathscr{P}$ denotes the principal value of the integral and $\omega = 2\pi c/\lambda$ the angular frequency. These relations (known also as the Tickmarsh theorem [16]) are valid for any linear response. (The only requirement is causality: the response must not come before the input.) The proof of the relations can be found in various places in different contexts (for instance [12,17]), [16] being the most general one. Using the symmetry properties

$$\delta_1(-\omega) = \delta_1(\omega),$$
$$\delta_2(-\omega) = -\delta_2(\omega) \tag{11}$$

and rewriting in terms of wavelength rather than frequency, one obtains the relation

$$\delta_2(\lambda) = \frac{2\lambda}{\pi}\mathscr{P}\int_0^\infty \frac{-\delta_1(\lambda')}{\lambda^2 - \lambda'^2}\,\mathrm{d}\lambda'. \tag{12}$$

δ_2 tends to be positive at the long-wavelength side, and negative at the short-wavelength side of an absorption line, similarly to the behavior found in Appendix A for a single absorption line.

We are interested in δ_2 in the visible range, but, according to eq. (12), it gets contributions from absorption bands at other wavelengths. We split the imaginary reemission coefficient accordingly,

$$\delta_2(\lambda) = \delta_2^0 + \delta_2^{\mathrm{vis}}(\lambda), \tag{13}$$

where δ_2^{vis} is the contribution of the visible absorption lines of the pigments in the membrane, while δ_2^0 is the consequence of the absorption lines outside of the visible region.

The dashed line in fig. 3 shows δ_2^{vis} (together with the absorption) as calculated by restricting the integration in eq. (12) to the visible range $\lambda \in [350\ \mathrm{nm}, 700\ \mathrm{nm}]$. The absorption curve has

Fig. 2. The amplitude (E) of the resultant electromagnetic wave in front of and behind an infinite thin sheet as a function of the distances (z) from the sheet. (a) $\phi = -\pi$ (within the absorption band). (b) $\phi = -\pi/2$ ($\omega < \omega_0$). (c) $\phi = \pi/2$ ($\omega > \omega_0$). (Dotted line: the amplitude of the incident light propagating from the left to the right. In the horizontal axis the unit is the wavelength in the aqueous medium. The sheet is located at $z = 0$. $r = 0.15$). Amplitude (E) is shown relative to that (E_0) of the incident light. Calculated from eq. (9).

two distinct peaks. Both of them have a contribution to δ_2^{vis} similar to δ_2 calculated for a single absorption line in Appendix A. δ_2^{vis} gets a positive contribution on the long-wavelength side of an absorption peak and a negative one on the other side. Consequently, it has two positive peaks shifted to longer wavelengths comparing to the absorption peaks and it is negative at the blue end of the spectrum. Between the two absorption maxima it gets opposite contributions from the two absorption peaks, so it is small, but happens to remain positive.

According to eq. (B.8)

$$\delta_2^0 = (n-1)k_w a, \tag{14}$$

where n is the refractive index of the pigment-free membrane relative to the surrounding medium and a is the membrane thickness. We suppose, that n is approximately wavelength independent in the visible region. (This is true, if the relevant absorption lines are not very close to the visible region.)

2.4. *Light distribution in the stroma-thylakoids*

The stroma-thylakoid consists of pairs of adjacent membrane sheets (fig. 4). The question is which of the two sheets receives more light than the other when they are illuminated perpendicularly.

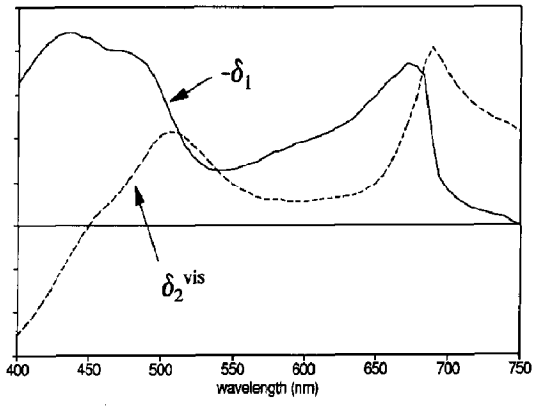

Fig. 3. The reemission coefficients as a function of the wavelength. Continues line: $|\delta_1|$ (absorption, experimental) and dashed line: the visual contribution to the reemission coefficient δ_2^{vis}, as calculated from eq. (12) restricting the integration to the visible wavelength range 350–750 nm.

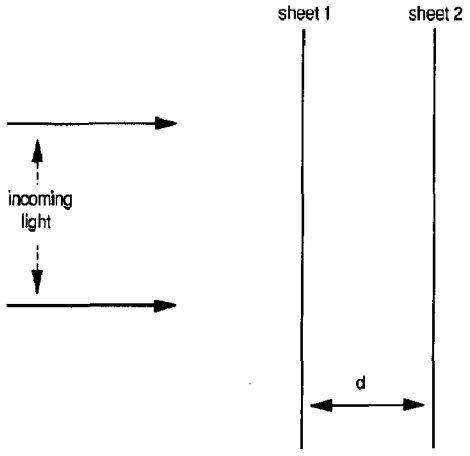

Fig. 4. Stroma-membrane geometry.

Above, the interaction of light with a single infinite sheet was discussed. One can calculate the light amplitude at either sheet as a superposition of the original incident light and the light re-emitted by the other sheet. Because of the weakness of the interaction ($r \ll 1$) one may use the amplitude of the original incident light to calculate the light re-emitted by the second sheet rather than taking into account that the first sheet also modifies the light amplitude at the second sheet. (We neglect the possibility that a photon can be scattered more than once before its final absorption.)

According to eq. (9) (with $z > 0$), the amplitude of light at the sheet in the "shadow" of the other one, is

$$|E_2| = E_0(1 + r\cos\phi) = E_0(1 - |\delta_1|) \tag{15}$$

as a consequence of presence of the other sheet. That $|E_2| < E_0$ (eq. (15)), reflects the shading effect of the classical light-gradient theory [4,5]. The sheet nearer to the light source experiences an amplitude (from eq. (9), $z = -d$)

$$\begin{aligned} |E_1| &= E_0[1 + r\cos(\phi + 4\pi n_w d/\lambda)] \\ &= E_0[1 - |\delta_1|\cos(4\pi n_w d/\lambda) \\ &\quad -\delta_2 \sin(4\pi n_w d/\lambda)], \end{aligned} \tag{16}$$

where d is the distance between the two sheets. (eq. (5) was used.) The first term (E_0) may be ascribed to unperturbed incident light. The two other terms are due to light back scattered from the second sheet, both the in-phase and the out-of-phase reemission having a respective contribution.

The relative light intensity difference (light gradient) between the sheets is

$$\left(\frac{\Delta I}{I_0}\right)_{\text{stroma}} = \frac{|E_1|^2 - |E|_2^2}{|E|_0^2}$$
$$= 2\{|\delta_1|[1 - \cos(4\pi n_w d/\lambda)] - \delta_2 \sin(4\pi n_w d/\lambda)\}, \quad (17)$$

where I_0 is the incident intensity. ($r \ll 1$ was used.) The first term (which is proportional to the light absorption) has two components: the former ("1") comes from the shading while the latter is due to the interference between the incident and the back-scattered light. In total, the first term is always positive: absorption (in-phase reemission) leads to a "normal" light gradient. But this light intensity difference is smaller than predicted by the shading alone. The second term is a pure interference term. It is positive at the short wavelength side of a single absorption line (where δ_2 is negative), but negative at the long wavelength side. Consequently, the out-of-phase reemission leads to an "inverse" light gradient at the long-wavelength side of an absorption peak.

For

$$d \ll \lambda \quad (18)$$

(which is realistic for the chloroplasts) we can use a Taylor expansion of eq. (17):

$$\frac{\Delta I}{I_0} \approx -8\pi n_w \delta_2 \frac{d}{\lambda} + 16\pi^2 n_w^2(-\delta_1)\left(\frac{d}{\lambda}\right)^2. \quad (19)$$

The light intensity difference between the sheets becomes zero at zero distance. (This phenomenon is related to the fact mentioned at eq. (9), i.e. that the light intensity is the same immediately in front of and behind a single sheet.)

Our second observation concerning eq. (19) is, that the leading (linear in d/λ) term comes from δ_2 rather than from the absorption, i.e. from interference at the front sheet between the incident light and the light out-of-phase-reflected from the back sheet. For $d \ll \lambda$ this term is more important than the absorption at the front sheet. At the long-wavelength side of an absorption band $\delta_2 > 0$, making the leading term negative. (The reflection invokes a $\phi = 90°$ phase delay. At the front sheet the phase difference becomes larger than 90°, so the interference becomes destructive, because of the path length difference between the two light waves.)

Our conclusion is, that in the case of $\delta_2 > 0$, which obtains at wavelengths exceeding an absorption maximum, the front sheet of the stroma-thylakoid receives less light than the back sheet. This situation leads to an inverse polarity of the photovoltaic effect compared to what would be expected from the original version of the light gradient theory.

2.5. Light distribution in the grana-stacks

We will approximate the grana-stack as a single homogenous sheet with thickness D rather than handle all of the membrane sheets separately (fig 5). This is possible because the distance between its thylakoid lamellae is much smaller than the wavelength. A short calculation establishing this approximation in more quantitative

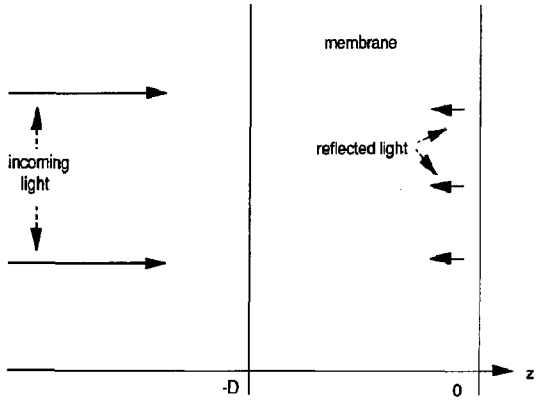

Fig. 5. Grana geometry.

terms is presented in Appendix C. The light intensity pattern is determined by absorption as well as by the reflections at the front and back surfaces of the grana-stack.

According to Appendix B, the (average) complex refractive index of the grana-stack (relative to the aqueous medium):

$$n = 1 - i\frac{l\delta}{k_w}, \tag{20}$$

where l is the number of membrane sheets per unit distance perpendicular to the sheets. The complex wave number of the light in the grana-stack:

$$k_g = nk_w. \tag{21}$$

The real part of k_g (k_1) is the wave number in the usual sense, while its imaginary part (k_2) is half the absorbance [12]. The reflection coefficient α (in terms of the amplitudes rather than the intensities) at the surfaces, if the light derives from the grana region [12] equals

$$\alpha = \frac{n-1}{n+1}. \tag{22}$$

According to Appendix D, the interference pattern is the following:

$$E = \frac{e^{ik_g z} + \alpha\, e^{-ik_g z}}{1 - \alpha^2\, e^{2ik_g D}} E_0 \approx (e^{ik_g z} + \alpha\, e^{-ik_g z}) E_0. \tag{23}$$

($z = 0$ at the back surface of the grana as shown in fig. 5. E_0 is measured here.) Only the numerator depends on the position. It corresponds to a standing wave interference between the incident light and the light reflected from the back surface. The denominator (constant in space) is a consequence of the reflections back and forth. (It depends on the ratio of the grana thickness to the wavelength. The situation corresponds to a Fabry-Perrot interferometer.) If $|\alpha|$ is small (as in the present case), and only one reflection is important, the denominator is equal to 1. We will use this approximation.

Using the approximation $n - 1 \ll 1$, eq. (20) gives, for the real and the imaginary parts of the reflection coefficients, respectively:

$$\alpha_1 = \frac{l\delta_2}{2k_w},$$

$$\alpha_2 = \frac{l|\delta_1|}{2k_w}. \tag{24}$$

Eq. (23) leads to the following expression for the light intensity:

$$\begin{aligned}\frac{I(z)}{I_0} = \frac{|E|^2}{E_0^2} &\approx e^{-l|\delta_1|z} + |\alpha|^2\, e^{l|\delta_1|z} \\ &\quad + \frac{l}{k_w}[\delta_2 \cos(2k_1 z) + |\delta_1| \sin(2k_1 z)] \\ &\approx 1 - l|\delta_1|z + \frac{l}{k_w}[\delta_2 \cos(2k_1 z) \\ &\quad + |\delta_1| \sin(2k_1 z)],\end{aligned} \tag{25}$$

where I_0 is the attenuated incident intensity at the back surface and $I(x)$ is the intensity at the position x. $|\alpha| \ll 1$ was used once more, and the absorption term was linearized.

With respect to the photovoltage experiments we are interested in the sum of the light intensity differences across the individual thylakoid disks in the grana-stack,

$$\Delta I = \sum_{i=1} (I_{2i-1} - I_{2i}). \tag{26}$$

(I_k stands for the light intensity at the kth sheet. Sheets are indexed from the surface facing the light. ΔI is positive, if it leads to a positive photovoltage signal.) We calculate this sum using the light intensity values at the membrane sheets derived above from the continuous model of the grana. The light intensity changes approximately linearly with distances much smaller than the wavelength, so

$$I_{2i-1} - I_{2i} = \frac{d_{in}}{d_{bet}}(I_{2i} - I_{2i+1}), \tag{27}$$

where d_{in} and d_{bet} are the distance of the two sheets in one thylakoid vesicle and the distance between two adjacent vesicles, respectively. So

the light intensity difference we are interested in, is proportional to the light intensity difference between the front and the back surface,

$$\begin{aligned}\Delta I &\approx \sum_{i=1}^{n} (I_{2i-1} - I_{2i}) \\ &= \frac{\sum_{i=1}^{n} (I_{2i-1} - I_{2i}) + \sum_{i=1}^{n} (I_{2i} - I_{2i+1})}{\gamma} \\ &= \frac{\sum_{i=1}^{2n-1} (I_{i+1} - I_i)}{\gamma} = \frac{I_1 - I_{2n}}{\gamma} \\ &= \frac{I(-D) - I(0)}{\gamma}, \end{aligned} \tag{28}$$

where

$$\gamma = 1 + \frac{d_{\text{in}}}{b_{\text{bet}}}. \tag{29}$$

Combining eqs. (25) and (28) one obtains:

$$\begin{aligned}\left(\frac{\Delta I}{I_0}\right)_{grana} \approx \big(&2l|\delta_1|D - (l/k) \\ &\times \{\delta_2[1 - \cos(2k_1 D)] \\ &+ |\delta_1|\sin(2k_1 D)\}\big)\gamma^{-1}. \end{aligned} \tag{30}$$

$d_{\text{in}} = d_{\text{bet}}$ and, consequently, $\gamma = 2$ will be used in the following.

The first term corresponds to the simple absorption phenomena, while the other two terms have a wave-optics origin. Obviously, the first term dominates the formula for large D. In other words, grana follows geometrical optics, if the thickness is not small compared to the wavelength.

2.6. *Prediction of the polarity of the macroscopic photovoltage*

Far below the saturating light intensity the photovoltage is proportional to both the light intensity difference and the absorption at the given wavelength:

$$\Delta U \sim |\delta_1|\Delta I. \tag{31}$$

To make the grana- and stroma-membrane predictions comparable we use a value relative to the area A of the membrane involved in the generation of the signal. In the stroma-thylakoids two layers are involved, while in the grana the number of layers is lD. Consequently, the relative photovoltage for the stroma-thylakoid and the grana can be written as

$$\begin{aligned}\frac{\Delta U_{\text{stroma}}}{A_{\text{stroma}}} &\sim \frac{|\delta_1|\Delta I_{\text{stroma}}}{2}, \\ \frac{\Delta U_{\text{grana}}}{A_{\text{grana}}} &\sim \frac{|\delta_1|\Delta I_{\text{grana}}}{lD}. \end{aligned} \tag{32}$$

Note, that l drops from $\Delta U_{\text{grana}}/A_{\text{stroma}}$ because eq. (30) is proportional to l.

We have two geometrical parameters to estimate: d, the distance between the stroma-membrane sheets, and D, the grana thickness. The thickness of the thylakoid membrane is 7 nm [1]. In the EM pictures (see for instance ref. [2]) the inner space of the stroma-thylakoid has the same thickness as the membrane itself. This suggests the distance between the central planes of the membrane sheets to be 14 nm. (We cannot be sure whether the fixation procedure necessary to take the EM picture affects this distance.) The grana thickness varies. The value $D = 200$ nm is chosen as representative according to the EM pictures [2].

There is a third parameter to estimate: the relative strength of the two origins of the reemission constants. (Remember that δ_1 and δ_2^{vis} are related to the absorption lines in the visible region, while δ_2^0 is related to the absorption lines outside this region. Obviously, multiplying all of the δ by a constant factor does not modify the light distribution pattern.)

According to ref. [1], there are around 10^5 pigment molecules for each thylakoid disk, with 500 nm in diameter. This amounts to 2×10^{13} pigment molecules/cm^2 surface density, and $|\delta_1| \approx 10^{-3}$ around 650 nm. Choosing $n - 1 \approx 0.01$ (that is, supposing, that the refractive index of the thylakoid membrane differs only slightly from the aqueous medium) leads to a similar value for δ_2^0 (eq. (14)).

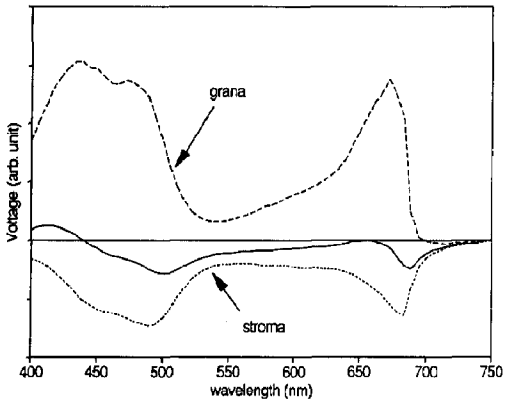

Fig. 6. Predicted action spectra of the photovoltaic signal. Dotted line: stroma-thylakoid; dashed line: grana; continuous line: a linear combination of the two with weight 0.25 and 0.75, respectively.

Fig. 6 shows the expected action spectrum for the stroma-thylakoid as well as the grana for the parameter values mentioned above. As a general rule, the expected signal from the stroma-thylakoid is negative, while the expected signal in the grana is positive. In the region of short wavelengths the stroma signal becomes positive, too. The grana curve follows the absorption. Compared to the positive grana peaks the two negative peaks of the stroma signal are shifted to the direction of the longer wavelengths. (This is a consequence of the behavior of the imaginary part of the reemission coefficient near to an absorption band, as mentioned before.)

The linear combination of the expected grana and the expected stroma photovoltaic effects is similar to the experimental results as summarized in fig. 3 of ref. [11]. See section 3 for a detailed comparison.

3. Discussion

In this paper we have calculated the implications of optical interference for the macroscopic voltage generated by a suspension of chloroplasts. The results explain the hitherto ununderstood features of the experimental data, i.e. inverse polarity and wavelength dependence.

Perhaps a simpler way to explain the wavelength dependence of the photovoltaic effect would have been to consider the changing ratio between the wavelength and the geometrical distances in the system. But the complicated form of the wavelength dependence makes this possibility unlikely. The observed relationship between the photovoltage action spectrum and the absorption spectrum [11] suggests the relevance of the phase of the reemitted light, while the kinetic difference between the positive and the negative experimental signals suggests different structural origins for the two types of signal. The present paper demonstrates, that these two factors together can explain the basic properties of the effect.

It is worthwhile to note, that the circular dichroism spectrum of thylakoids also has a wavelength dependence seemingly connected to the real and imaginary part of the reemission [20,21].

Fig. 6 shows that the grana signal is expected to be positive, while the stroma signal is expected to be negative except at the blue end of the spectrum. Comparing this result to the fact [11], that the positive signals have a slow decay component, while the negative ones do not, we conclude that only the grana signals have this slow component. Decay of the signal is usually attributed to ion relaxation around the thylakoid system. A possible explanation of the difference in relaxation times may be the restricted mobility of the ions between the appressed membrane regions in the grana stack.

For photovoltaic experiments the two most frequently used light sources have been the frequency-doubled Nd–YAG laser and the ruby laser with wavelengths 530 and 694 nm, respectively. (See for instance the investigations in refs. [9,10,18,19].) At these wavelengths the grana signal is expected (cf. fig. 6) to be negligible, and only the fast, negative stroma signal should contribute. This conclusion is in accordance with the observed polarity [9]. (Investigations with these two types of laser led to the controversial conclusion, that the laser generated signals are different from the ones generated by flash lamps [9]. But different experiments with different types of lasers [7,11] have since excluded this proposition.)

It was an important observation by Trissl et al. [18,19], that under stacking conditions only the PSI contributes to the photovoltage, while both of

the photocenters do so under destacking conditions. These workers explained this observation by the delocalization of the excitation energy within PSII units in the grana stack. ("Excitonic short circuit".) Taking into account, that these observations [18,19] were made using a Nd–YAG laser, the present paper offers an alternative explanation: At the wavelength used, only the stroma-thylakoid generates photovoltage. PSII particles are present in the stroma-membranes only at destacking conditions [3].

The grana signal follows the absorption curve, because the leading term in eq. (30) comes from the absorption. It has two wide maxima around 420 and 660 nm (fig. 6, dashed line). This prediction agrees with the observations of slowly decaying positive signals at this wavelength region [7,8,11].

There are kinetic differences between the two peaks [11]: the signal generated by a 660 nm flash does not have a fast decay component, while the signal at 420 nm does. These differences can be explained by considering our results as presented in fig. 6 and the fact, that both stroma and grana-thylakoid are present in the experiments. Above we concluded, that whereas the photovoltage generated by the stroma-membranes decays quickly, more or less as a single component, the photovoltage generated by the grana decays by both a quick and a slow component. In a macroscopic mixture we should thus expect photovoltaic signals with a slow decay component to follow the action spectrum predicted for the grana stacks (i.e. the dashed line in fig. 6). Photovoltaic signals with rapid decay should follow some wavelength-independent linear combination between the stroma (dotted line in fig. 6) and the grana (dashed line in fig. 6) action spectra. The full line in fig. 6 is one possible linear combination (with relative weights 0.25 and 0.75 for the grana and for the stroma-thylakoid). More specifically, at 420 nm one should expect a strong slow and a strong rapid component, i.e. a positive signal with biphasic decay. At 660 nm, where the full line in fig. 6 is nearly zero, one should expect a slow positive component, with very little fast component.

There is a wide wavelength region around 600 nm in which the predicted grana signal (that is the slow component) is positive, while the sum (predicting the fast component) is negative. In that region our theory predicts a signal with an alternating sign: a fast negative peak is followed by a slow negative one. These predictions fully agree with the measurements [8,11].

The relative weights underlying the full line in fig. 6, are arbitrary. The ratio between the membrane types is variable and even depends on the light adaptation. So we cannot expect that any experiment with different species and/or different experimental conditions reproduces the lack of the fast component close to the red absorption maximum. The important point is, that we can interpret even the kinetic difference between the two positive signals generated by different wavelengths by taking into account the behavior of δ_2^{vis}.

In the calculations we did not take into account the minor difference between the action spectra of the two photocenters. It might be important at the red end of the visible spectrum, where the PSII stops to work at 680 nm, while PSI is active until 700 nm. This difference can contribute to the sharp polarity change at the red end of the visible spectrum, because the PSI located in the stroma-membrane generates negative signal.

A limitation of the work reported here is that it is restricted to membrane structure aligned perpendicularly to the light path. There are two observations on photovoltage signal from chloroplasts oriented parallel to the light path, both of them reporting slow positive signals [23,7]. Originally, it was argued, that these results exclude the light gradient explanation [23], but later they were explained within this framework [7]. We approximated the grana structure by a continuous medium. In this approximation it is quite obvious, that a similar signal should be generated in either orientation.

We approximated the stroma membranes by infinitely thin parallel sheets. This approximation could be questioned on the basis, that the distance between the membrane sheets is similar to the membrane thickness. An alternative approach would be to consider the reflections on both of

the surfaces of every membrane sheet. (Such a kind of calculation was carried out in ref. [24].) However, interference between the two reflections gives the same wave as calculated here using the reemission coefficient, if the membrane thickness is much smaller than the wavelength. With this condition, the real membrane is equivalent to an infinitely thin sheet having the same reemission coefficient and located at the mediator plane of the membrane. The validity of this approach is independent of the distance between the membranes.

An important shortcoming of our theory might be that in reality the pigments are not distributed continuously in the thylakoid membrane but located in pigment–protein complexes in a well-defined order. The characteristic scale is in the same order of magnitude as the distance between the sheets: nanometers. Moreover, the distribution of the complexes in two adjacent membranes are not independent from each other. (For instance, interactions between the light harvesting complexes play an important role in membrane stacking [25].) There are no simple ways to deal with these spatial inhomogeneities.

Pigments do not interact with the light independently. (See ref. [26] for the general theory.) The interactions between the pigments within a single membrane sheet are not a problem, because the only consequence of such a kind of interaction is a change in the absorption spectrum of the sheet and we used the empirical spectrum. (The Kramers–Kronig relations remain unchanged.) The situation is different for the interaction between the pigments of two different membrane sheets. Such an interaction leads to a spectrum depending on the inter-membrane distance. The fact, that no geometry dependence of the spectrum is known, suggests that neglecting this interaction is a justified approximation. (Following ref. [26] there is a way to take into account the interaction of homogeneous sheets, but, because of the above-mentioned lack of homogeneity, we considered the implementation irrelevant for the present study.)

We made a distinction between two sources contributing to the reemission coefficient. δ_1 and δ_2^{vis} come from the visible absorption peaks of the pigments and can be calculated from the visible absorption spectrum, while δ_2^0 comes from the absorption peaks outside the visible range and can be calculated from the refractive index of the pigment-free membrane. The ratio between these two components is a crucial parameter of the present theory. We supposed, that both of them have a contribution in the same order of magnitude.

Unfortunately, the refractive index of a membrane is hard to measure directly. An estimation based on the refractive index value of oil droplets from natural sources gives a value between 1.45 and 1.52 for the refractive index of a biological membrane [24]. It corresponds to a refractive index around 1.1 relative to that of pure water. Using this value for n rather than the 1.01 we did use, δ_2^0 should dominate δ_2^{vis} by an order of magnitude, leading to a prediction of an almost wavelength-independent negative stroma signal. That prediction contradicts the experimental facts quite strongly, as positive signals are observed most definitely. We interpret this discrepancy as a result of oversimplification: a thylakoid membrane is far from an oil droplet. In fact, thylakoid membrane contains virtually equal amounts of lipid and proteins, as well as a considerable amount of water. Moreover, the water between and around the membranes is full of proteins. A 0.4 M sucrose concentration alone increases the refractive index of the aqueous medium from 1.333 to 1. 352 [27]. Consequently, the difference in refractive index between the thylakoid membranes and the medium between them may indeed be as small as only a few percent.

There are a few other problems making the ratio between the two components uncertain:

– There is an uncertainty in the estimation of the pigment content.

– The problem of inhomogeneity affects the two components differently, because one of the components is connected to the pigments, while the other one comes from all of the molecules.

– It is not clear, whether refractive index measurements on isotropic samples are relevant for the bimolecular liquid-crystal structure of a membrane or the partially ordered water structure between the membranes.

We conclude, that the qualitative features of the wavelength-dependent photovoltaic effects observed in chloroplast suspensions can be explained by our theory. Understanding of the phenomena in all its quantitative aspects however, requires more experimental as well as theoretical investigations.

The optical interference effects reported here may have functional implications. It remains to be seen if perhaps the thylakoid structure in chloroplasts is optimal with respect to the light intensity pattern.

After submitting this article we were attended to the paper of Paillotin et al. [28]. In this work a similar theory was developed for the light distribution in the stroma-thylakoid. These authors prefer to use reflections from the two sides of a membrane sheet rather than reemissions from the membrane material, which is an equivalent formulation of the same physics. The important difference between the two approaches is, that Paillotin et al. intend to explain the positive as well as the negative signals by light intensity difference between the two membrane sheets of the stroma-thylakoid. To get the prediction of positive signals within the absorption bands they use different numerical values than we did and assume a smaller dielectric constant inside the thylakoid vesicle, then outside.

Appendix A. The frequency dependence of the reemission coefficient calculated for a single absorption line

In this Appendix we calculate $\delta(\omega)$ for the case of only one absorption line as an illustration. (ω denotes the circular frequency of the light.) We use a treatment of the radiation of an infinite sheet developed by Feynman and Orear [13] which saves us from complicated integrations.

Let $\kappa(\omega)$ be the frequency-dependent complex polarizability of the membrane. (More exactly, the excess polarizability of the membrane over the polarizability of the reference aqueous medium around the membrane taken into account by the reference medium refractive index n_w.) If the density of induced dipoles is $d = \kappa E_{in}$, the current density (current per unit distance in the Y direction) is

$$j = \dot{d} = \kappa \dot{E}_{in} = -i\omega\kappa E_{in}. \tag{A.1}$$

This current radiates electromagnetic waves to the $+z$ as well as to the $-z$ direction with the same amplitude. The Maxwell equation

$$\mathrm{rot} H = \frac{4\pi}{c} J + \epsilon \frac{\partial E}{\partial t} \tag{A.2}$$

implies [13], that at the plane of the sheet the magnetic field, H of this outgoing radiation at $z = 0$ is

$$2|H_{out}| = 4\frac{\pi}{c}|j|. \tag{A.3}$$

(One has to regard a rectangular closed curve around j. The magnetic field of the outgoing radiation is opposite on the two sides of the membrane sheet. This discontinuity is connected to the electrical current in the sheet. CGS units are used. c is the velocity of light in vacuo.) It implies for the outgoing electric field at $z = 0$:

$$E_{out} = -\frac{2\pi}{cn_w} j. \tag{A.4}$$

Consequently the radiated field is:

$$E_{out} = \delta\, e^{-i(\omega t + k|z|)} E_{00} = \delta\, e^{k|z|} E_{in}, \tag{A.5}$$

where

$$\delta = i\omega \frac{2\pi}{cn_w} \kappa. \tag{A.6}$$

(δ is real if the polarizability is purely imaginary, and vice versa.)

Let us suppose, that the polarizability can be modeled by one classical oscillator with resonance frequency ω_0 and damping factor s. The $x(t)$ displacement of the electric charge satisfies the equation.

$$\ddot{x} + s\dot{x} + \omega_0^2 x = \frac{q}{m} E_{in} \tag{A.7}$$

where q and m represent the charge and the mass of the electron, respectively. The solution is:

$$x = \frac{q/m}{\omega_0^2 - \omega^2 - s\omega i} E_{in} \tag{A.8}$$

The complex polarizability is

$$\kappa = \frac{\eta q x}{E_{\text{in}}} = \frac{\eta q^2}{m} \frac{1}{\omega_0^2 - \omega^2 - s\omega \mathrm{i}}, \tag{A.9}$$

where η is the number of dipoles per unit area. The real and imaginary part of δ then become:

$$\text{Re } \delta = -\frac{2\pi\eta q^2}{mv} \frac{s\omega^2}{\left(\omega_0^2 - \omega^2\right)^2 + s^2\omega^2} < 0,$$

$$\text{Im } \delta = \frac{2\pi\eta q^2}{mv} \frac{\left(\omega_0^2 - \omega^2\right)\omega}{\left(\omega_0^2 - \omega^2\right)^2 + s^2\omega^2}. \tag{A.10}$$

This shows, that the reemission coefficient is strongly frequency dependent around the resonance frequency. The real part (always negative) represents the absorption. It has an extreme at the resonance frequency. The imaginary part representing the out-of-phase reemission changes sign at this frequency. (The connection between the out-of-phase reemission and the refractive index is discussed in the next Appendix.) These features remain unchanged for the general case according to the Kramers–Kronig relations. (See the main text.)

Appendix B. Connection of the reemission coefficient to the absorbance and the refractive indices

To clarify the relation of the reemission coefficient to the absorbance and refractive indices we investigate the propagation of the light through a continuous medium that will be regarded as a set of consecutive sheets. Let l be the number of sheets per unit length in the z direction. The electric field behind the sheet at a distance z (from repeated application of eq. (7)):

$$E(z) = E_0(1+\delta)^{lz}\, \mathrm{e}^{\mathrm{i}k_w z}, \tag{B.1}$$

where k_w represents the wave number in the (nonabsorbing) reference medium. (k_w is real.) If $|\delta| \ll 1$ as we suppose,

$$(1+\delta)^{lz} = \mathrm{e}^{l\delta z} \tag{B.2}$$

so that

$$E(z) = E_0\, \mathrm{e}^{\mathrm{i}k(1-\mathrm{i}l\delta/k_w)z}. \tag{B.3}$$

One can compare this expression with the following one describing light propagation in a medium with the complex refractive index n relative to the reference medium:

$$E(z) = E_0\, \mathrm{e}^{\mathrm{i}nk_w z} \tag{B.4}$$

(For real n, eq. (B.4) describes wave propagation with velocity v/n, where v is the velocity in the reference medium.) The comparison gives the relation

$$n = 1 - \mathrm{i}\frac{l\delta}{k_w}, \tag{B.5}$$

One can separate the real and the imaginary part of n:

$$E(z,t) = E_0\, \mathrm{e}^{l\delta_1 z}\, \mathrm{e}^{\mathrm{i}k(1+l\delta_2/k_w)z}, \tag{B.6}$$

from which one obtains the absorption coefficient as

$$\frac{\mathrm{d} - \ln(E/E_0)^2}{\mathrm{d}z} = -2l\delta_1 = 2k_w \text{ Im } n. \tag{B.7}$$

The real part of the refractive index is related to the imaginary part of the reemission coefficient δ by

$$\text{Re } n = 1 + \frac{l\delta_2}{k_w}. \tag{B.8}$$

It is important to stress, that n refers the refractive index relative to the nonabsorbing reference medium, in which k_w is measured.

Appendix C. The repeated sheets concept of the grana stack compared with the quasi-homogeneous concept

Here we present a calculation checking whether eq. (30) remains valid if we regard the grana stack a set of thin sheets rather than a continuous medium described by a refractive index. l is the number of sheets per unit length. For simplicity we will use the approximation that the contribution of the sheets are additive, that is we calculate the reflection from the sheets using for every sheet the same value for incident intensity. This is the same approximation as was used to calculate the light intensity in the stroma-thylakoid.

The interference terms of eqs. (25) and (30) comes from reflexions from the sheets. The sum of the reflected waves at the position z can be calculated as a geometric series,

$$E_{\mathrm{refl}}(z) = E_0 \sum_{j=1}^{l(-z)} \delta\, \mathrm{e}^{2ikaj} = \frac{\delta q}{1-\mathrm{e}^{2ika}}(1-\mathrm{e}^{-2ikz})E_0 \qquad \text{(C.1)}$$

(z is located at the back surface of the grana stack. E_0 is measured here.) Using the fact, that the distance between the lamellas are much smaller than the wavelength, that is $ka \ll 1$:

$$E_{\mathrm{refl}}(z) = \frac{1}{2k}\{(-\delta_1)\sin 2kz + \delta_2[1-\cos(2kz)]\}E_0. \qquad \text{(C.2)}$$

This formula leads to the interference terms of eqs. (25) and (30).

There is no doubt, that the absorption term is also the same in the two cases.

Appendix D. The interference pattern eq. (23) in the grana

Let us first consider the light waves that have suffered an even number of reflections. They propagate in the positive direction. The electric field of the wave that has experienced $2m$ reflections is:

$$E_{2m} = \alpha^{2m}\, \mathrm{e}^{ik(z+2mD)}E_0. \qquad \text{(D.1)}$$

This equations derives from the considerations that this wave has travelled a longer path to the point z than the incident one by $2mD$ and that every reflection contributes by a factor of α. As a consequence of eq. (D.1), the sum of the waves reflected an even number of times (including the incident one with $m = 0$),

$$E_{\mathrm{even}} = \left(\sum_{m=0}^{\infty}(\alpha^2\, \mathrm{e}^{2ikD})^m\right)\mathrm{e}^{ikz}E_0 = \frac{e^{ikz}E_0}{1-\alpha^2\, \mathrm{e}^{2ikD}} \qquad \text{(D.2)}$$

($|\alpha| < 1$ was used.)

Any wave reflected $2m+1$ times propagates to the negative direction. It has a longer path to the point z than the wave reflected only once by $2mD$. Consequently, the contribution to the electric field is

$$E_{2m+1} = \alpha^{2m+1}\, \mathrm{e}^{ik(-z+2mD)}E_0. \qquad \text{(D.3)}$$

The sum of all waves with an odd number of reflections amounts to

$$E_{\mathrm{odd}} = \left(\sum_{m=0}^{\infty}(\alpha^2\, \mathrm{e}^{2ikD})^m\right)\alpha\, \mathrm{e}^{-ikz}E_0 = \frac{\alpha\, \mathrm{e}^{-ikz}E_0}{1-\alpha^2\, \mathrm{e}^{2ikD}}. \qquad \text{(D.4)}$$

The total electric field is

$$E = E_{\mathrm{even}} + E_{\mathrm{odd}} = \frac{\mathrm{e}^{ikz}+\alpha\, \mathrm{e}^{-ikz}}{1-\alpha^2\, \mathrm{e}^{2ikD}}E_0 \qquad \text{(D.5)}$$

Acknowledgement

The late professor Don DeVault was the originator of the idea that interference may have an impact on the light gradient polarity. The authors benefitted from discussions with Béla Böddi, Andrzej Dobek, Győző Garab, Klaas Hellingwerf, Douglas Kell, Tom Muller, Elemér Papp, Zoltán Szigeti and John Whitmarsh and from comments of an anonymous referee. For GM this work was supported by a grant OTKA 2999 from the Hungarian Science Foundation and by the Peregrinatio Foundation. HVW acknowledges support by the Netherlands Organization for Scientific Research (NWO).

References

[1] H.T. Witt, Biochim. Biophys. Acta 505 (1979) 355–427.
[2] J. Brangeon and L. Mustárdy, Biol. Cellulaire 36 (1979) 71–80.
[3] B. Anderson and J.M. Anderson, Biochim. Biophys. Acta 593 (1980) 427–440.
[4] C.F. Fowler and B. Kok (1974) in: Progress in Photobiology (G.O. Schenek, ed.), Deutsche Gesellschaft für Lichtforsung e. V., 417. Abstr.; Proceedings of the VIth

International Congress on Photobiology Bochum, Bochum, Germany (1972).
[5] C.F. Fowler and B. Kok, Biochim. Biophys. Acta 357 (1974) 308–318.
[6] H.T. Witt and A. Zickler, FEBS Letters 37 (1973) 307–310.
[7] G. Meszéna, E. Papp and Gy. Fricsovszky, Studia Biophysica 126 (1988) 77–86.
[8] P. Gräber and H.-W. Trissl, FEBS Letters 123 (1981) 95–99.
[9] H.-W. Trissl, U. Kunze and W. Junge, Biochim. Biophys. Acta 682 (1982) 364–377.
[10] G. Meszéna and D. DeVault, Photosynthesis research 22 (1989) 115–122.
[11] G. Meszéna, Biophys. Chem. 48 (1993) 315–319.
[12] J.D. Jackson, Classical electrodynamics (Wiley, New York, 1974).
[13] J. Orear Fundamental Physics (Wiley, New York, 1967).
[14] R. de L. Kronig, J. Opt. Soc. Am. 12 (1927) 547.
[15] H.A. Kramers, Phys. Z. 30 (1929) 52.
[16] E.C. Titchmarsh, Introduction to the theory of the Fourier-integral (Oxford Univ. Press, Oxford, 1937).
[17] D.B. Kell, R.D. Astumian and H.V. Westerhoff Ferroelectrics 86 (1988) 59.
[18] H.W. Trissl, J. Breton, J. Deprez and W. Leibl, Biochim. Biophys. Acta 893 (1987) 305–319.
[19] H.W. Trissl, W. Leibl, J. Deprez, A. Dobek and J. Breton, Biochim. Biophys. Acta 893 (1987) 320–332.
[20] Gy. Garab, R. Leegood, D.A. Walker, J.C. Sutherland and G. Hind, Biochemistry 27 (1988) 2430–2434.
[21] Gy. Garab, A. Faludi-Dàniel, J.C. Sutherland and G. Hind, Biochemistry 27 (1988) 2425–2429.
[22] R.C. Jennings et al., FEBS Letters 117 (1980) 332–334.
[23] J.F. Becker, N.E. Geacintov and D.E. Swenberg, Biochim. Biophys. Acta 503 (1978) 545–554.
[24] K.W. Foster and R.D. Smyth, Microbiol. Rev. (1980) 572–630.
[25] J. Barber, Photobiochem. Photobiophys. 5 (1983) 181–190.
[26] D. Keller and C. Bustamante, J. Chem. Phys. 84 (1985) 2961–2971.
[27] R.C. Weast, ed., CRC Handbook of Chemistry and Physics (CRC Press, Boca Raton, 1979).
[28] Paillotin, A. Dobek, J. Breton, W. Leibl and H.W. Trissl, Biophys. J. 64 (1993) 974–980.